Supplementary Material

Figures

LC-ESI-MS/MS method of Flavonoid extract of PP in -ve ionization approach

Flavonoids were pointed out from the flavonoid extract of PP with the aid of quantification of mass data. 3,7-Dimethylquercetin, Malic acid, Kaempferol-3-O-desoxyhexoside, 3'-Hydroxydaidzein, Chrysoeriol-7-O-glycuronyl, 3,7-Dimethylquercetin, Quercetin-3-malonylglucoside, Ferulic acid, Cafeic acid, Umbelliferone, [6]-gingerol and Glucose were pointed out from ginger extract in negative ionization approaches as shown in Table 7.

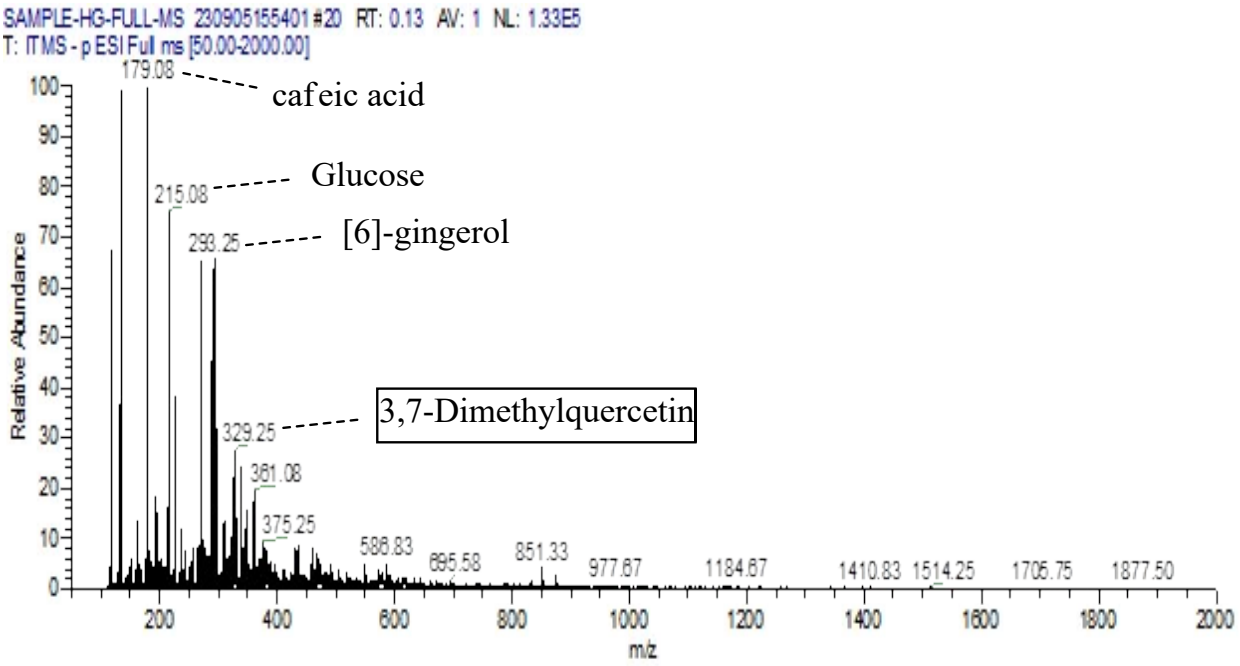

Figure S1. Comprehensive MS scale of total flavonoid from PP provoked utilizing $[M-H]^-$ ions

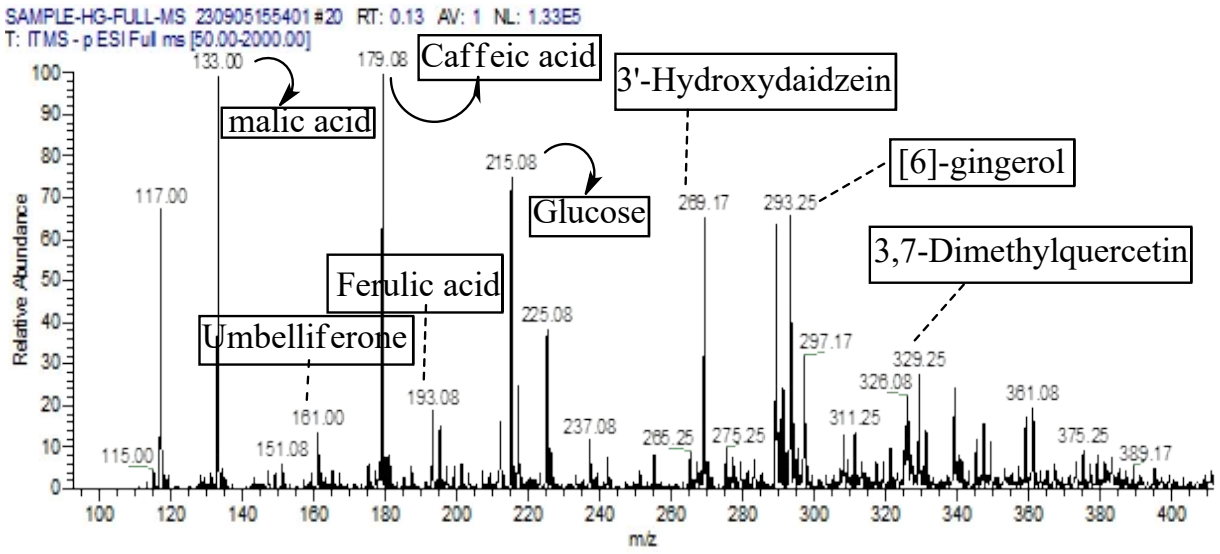

Figure S2. Comprehensive MS scale of total flavonoid from PP provoked utilizing $[M-H]^-$ ions.

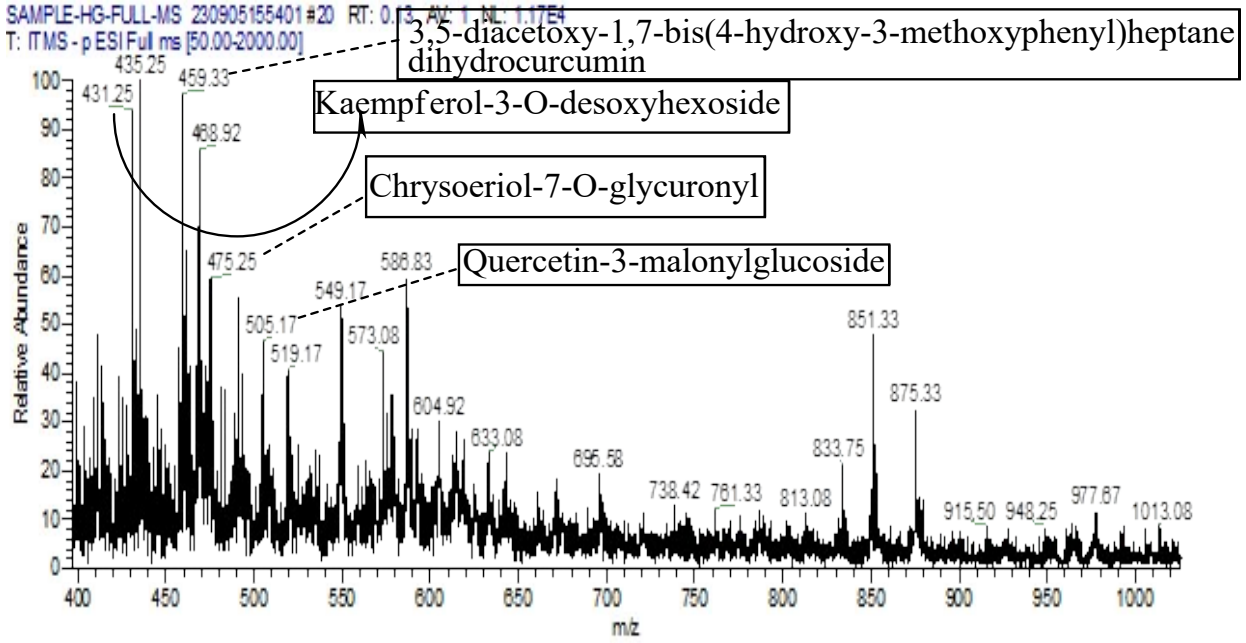

Figure S3 Comprehensive MS scale of total flavonoid extract from PP provoked utilizing $[M-H]^-$ ions.

The LC/ESI/MS/MS determination of vanilla of PP was studied in both +ve and -ve ionization approaches. The presence of a peak at m/z ratio 132.92 $[M-H]^-$ $C_4H_6O_5$ was pointed out as Malic acid in the mass spectrum of the negative ionization approach. The MS/MS scale showed the

fragmentation of the Malic acid peak at m/z 114.92 with the exclusion of $[M-H-H_3O]^-$ and at m/z 71.00 with the removal of $[M-H-CH_3O_3]^-$ (Figure S4).

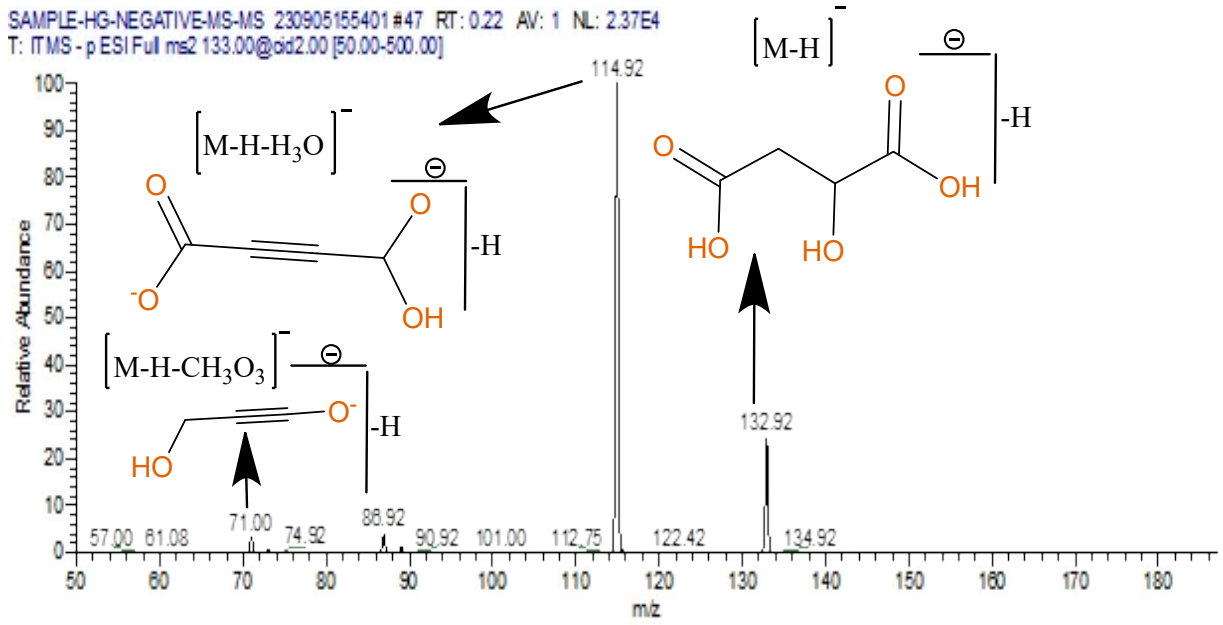

Figure S4 Comprehensive MS/MS spectra of Malic acid provoked utilizing $[M-H]^-$ ions

The appearance of a peak at m/z 161.00 $[M-H]^-$ $C_9H_6O_3$ was pointed out as 3-Hydroxycoumarin in mass spectra of the -ve ionization approach. The MS/MS range revealed the fragmentation of the 3-Hydroxycoumarin peak at m/z 146.08, corresponding to the exclusion of $[M-H-O]^-$, at m/z 100.00 with the removal of $[M-H-CH_2O_3]^-$ and m/z 80.92 with the removal of $[M-H-C_4H_2O_3]^-$ (Figure S5).

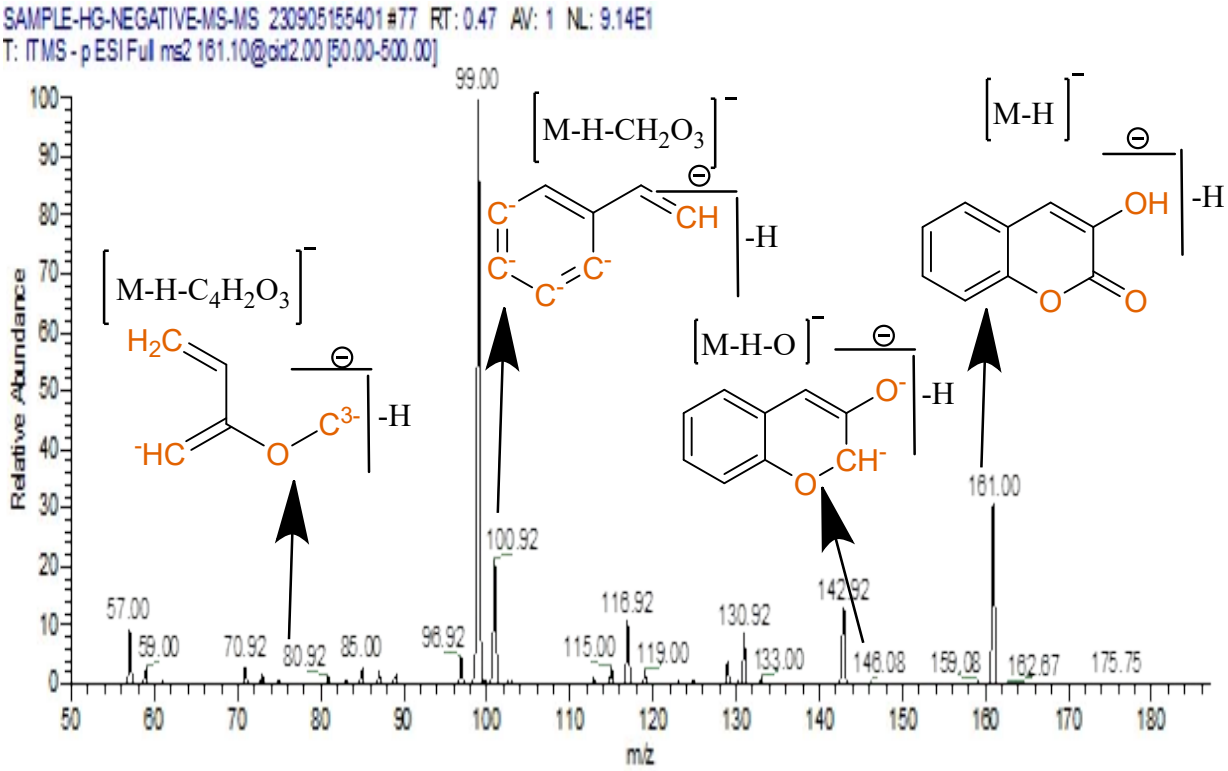

Figure S5 Comprehensive MS/MS spectra of 3-Hydroxycoumarin produced utilizing $[M-H]^-$ ions The precursor ion peak at m/z 179.00 $[M-H]^-$ $C_9H_8O_4$ was pointed out as Aspirin in the mass range of the -ve ionization approach. The MS/MS range exhibited the fragmentation of the Aspirin peak at m/z 161.08 with the extermination of $[M-H-H_3O]^-$, at m/z 124.92 with loss of $[M-H-C_2O_2]^-$ and at m/z 100.92 with loss of $[M-H-C_5H_4O]^-$ (Figure S6).

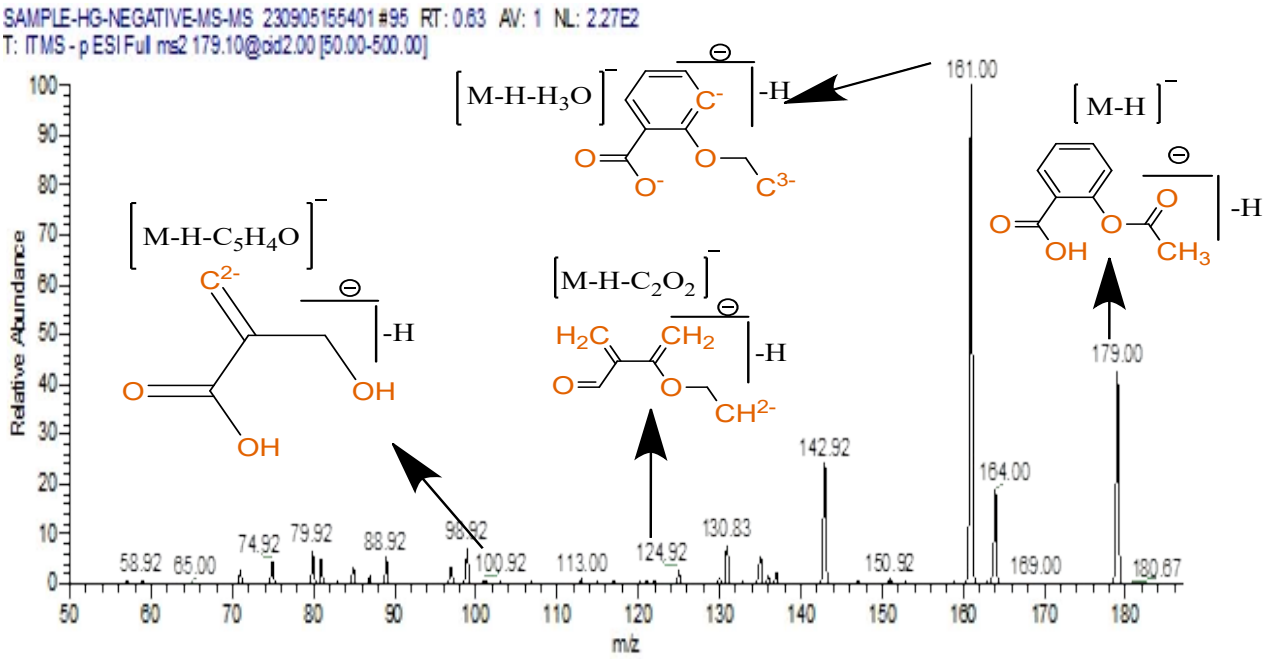

Figure S6 Comprehensive MS/MS range spectra of Aspirin provoked utilizing $[M-H]^-$ ions

The molecular ion peak at m/z 265.00 $[M-H]^-$ $C_{15}H_{22}O_4$ was revealed as Zinniol in the mass spectra range of the -ve ionization approach. The MS/MS spectra revealed the fragmentation of the Zinniol peak at m/z 221.08 with the extermination of $[M-H-C_3H_9]^-$, at m/z 136.92 with loss of $[M-H-C_8H_{18}O]^-$ and m/z 96.92 with the extermination of $[M-H-C_6H_{18}O_2]^-$ (Figure S7).also described by Jiang et al. [2].

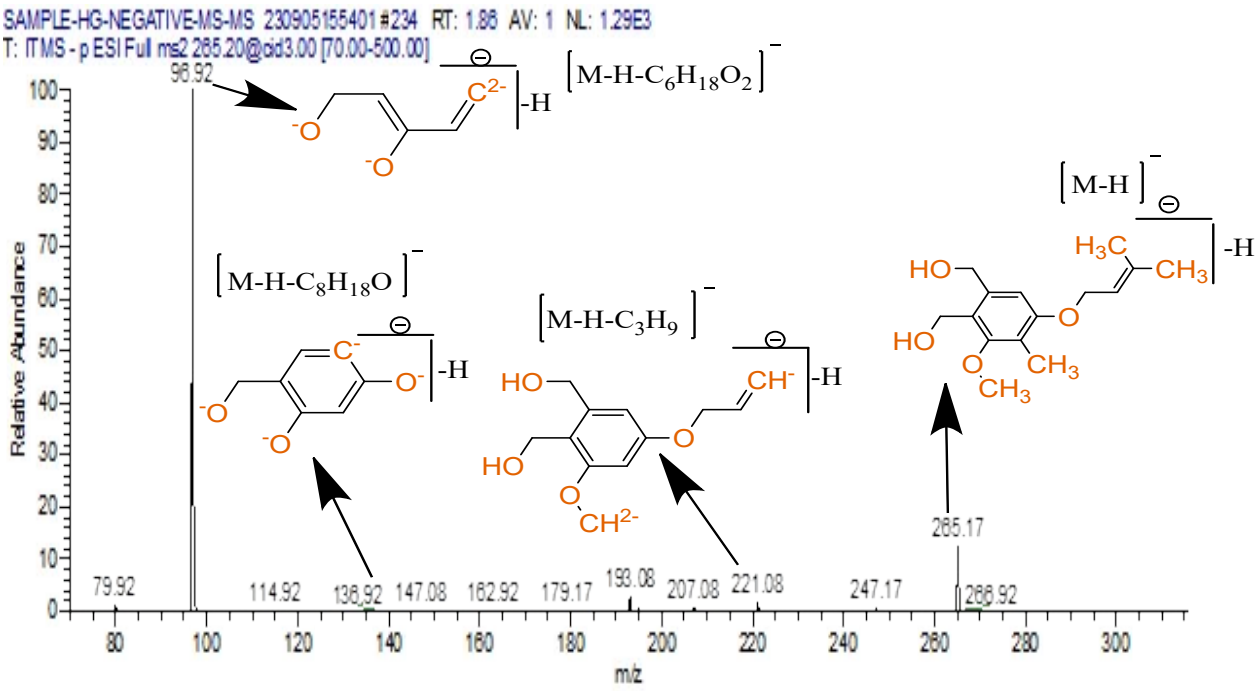

Figure S7 Comprehensive MS/MS spectral range of Zinniol provoked utilizing $[M-H]^-$ ions

The resulting ion sharp peak of product at mass/charge ratio 289.17 $[M-H]^-$ $C_{17}H_{22}O_4$ was determined as Tulipinolide in mass spectra range of -ve ionization approach. The MS/MS range showed the fragmentation of Tulipinolide peak at m/z 271.08 leads toward removal of $[M-H-CH_3]^-$, at m/z 149.00 with loss of $[M-H-C_7H_9O_3]^-$ and m/z 134.00 with extermination of $[M-H-C_8H_2O_3]^-$ (Figure S8).

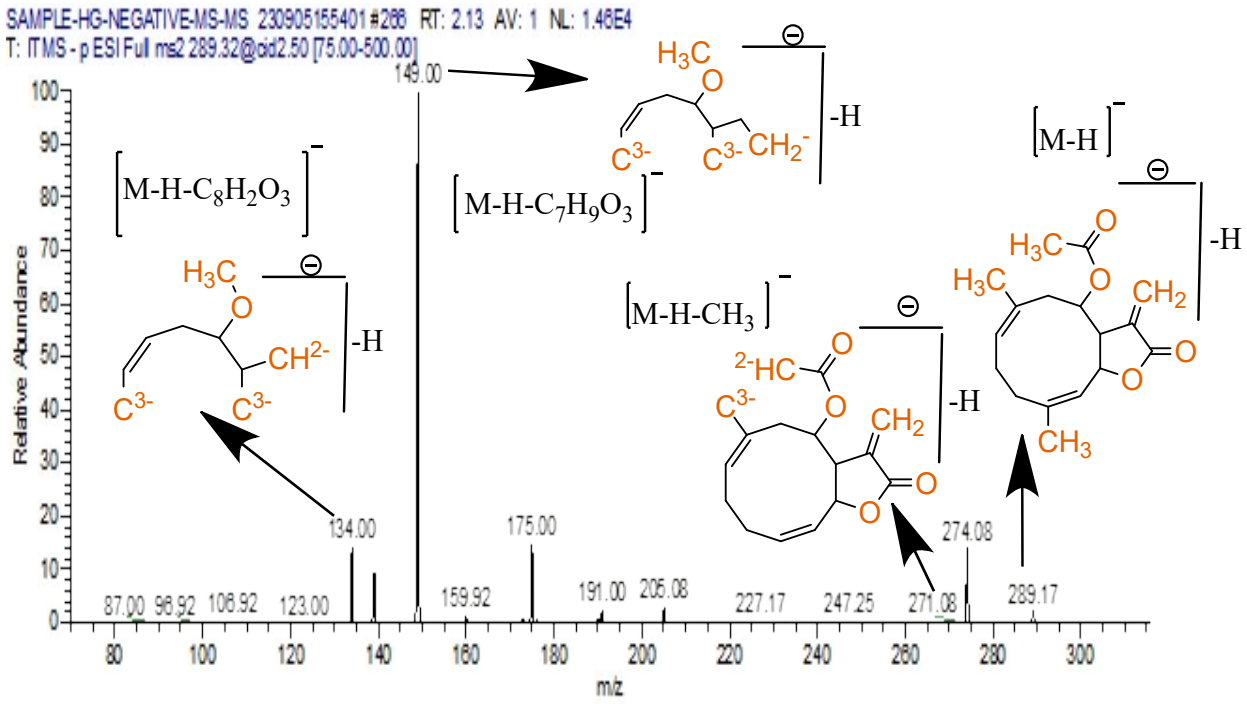

Figure S8 Comprehensive MS/MS scale of Tulipinolide produced utilizing $[M-H]^-$ ions

The ion peak of the product at m/z 293.17 $[M-H]^-$ $C_{17}H_{24}O_4$ was pointed out as Monoisononyl phthalate in the mass scale of the -ve ionization approach. The MS/MS spectrum exhibited the fragmentation of the Monoisononyl phthalate peak at m/z 278.17, corresponding to removal of $[M-H-CH_2]^-$, at m/z 193.08 with loss of $[M-H-C_7H_{15}]^-$, at m/z 178.00 with exclusion of $[M-H-C_{11}H_{18}]^-$ and at m/z 99.00 with removal of $[M-H-C_{13}H_{21}O]^-$ (Figure S9). also described by Tao et al.[3].

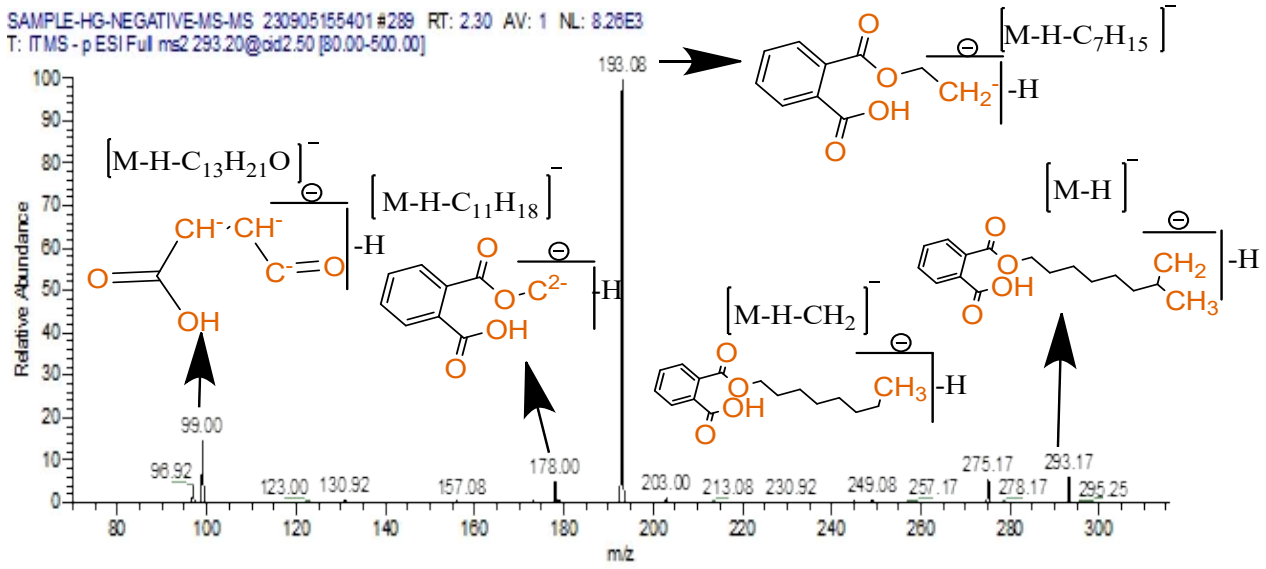

Figure S9 Comprehensive MS/MS scale of Monoisononyl phthalate produced using $[M-H]^-$ ions

The peak at m/z 321.17 $[M-H]^-$ $C_{19}H_{30}O_4$ was determined as 8-Gingerol in the mass scale of the -ve ionization approach. The MS/MS scale revealed the fragmentation of 8-Gingerol peak at m/z 221.00 by the removal of $[M-H-C_7H_{17}]^-$, at m/z 193.00 with loss of $[M-H-C_8H_{17}O]^-$ and m/z 127.00 with extermination of $[M-H-C_{12}H_{13}O_2]^-$ (Figure S10).

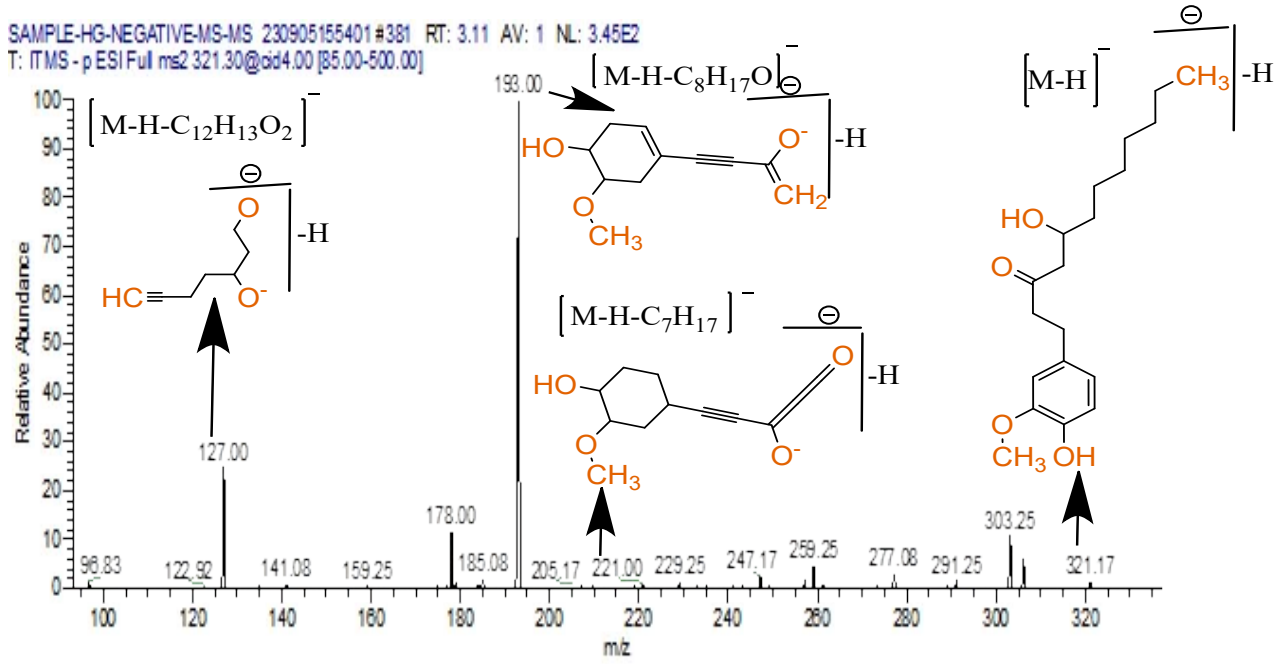

Figure S10 Comprehensive MS/MS scale of 8-Gingerol provoked using $[M-H]^-$ ions

The appearance of a peak at m/z 329.17 $[M-H]^-$ $C_{20}H_{26}O_4$ was determined as Carnosol in the mass scale of the -ve ionization approach. The MS/MS scale revealed the fragmentation of Carnosol peak at m/z 314.17 by the loss of $[M-H-CH_4]^-$, at m/z 207.08 with loss of $[M-H-C_6H_{19}O_2]^-$ and m/z 165.92 with the removal of $[M-H-C_7H_{25}O_3]^-$ (Figure 11).

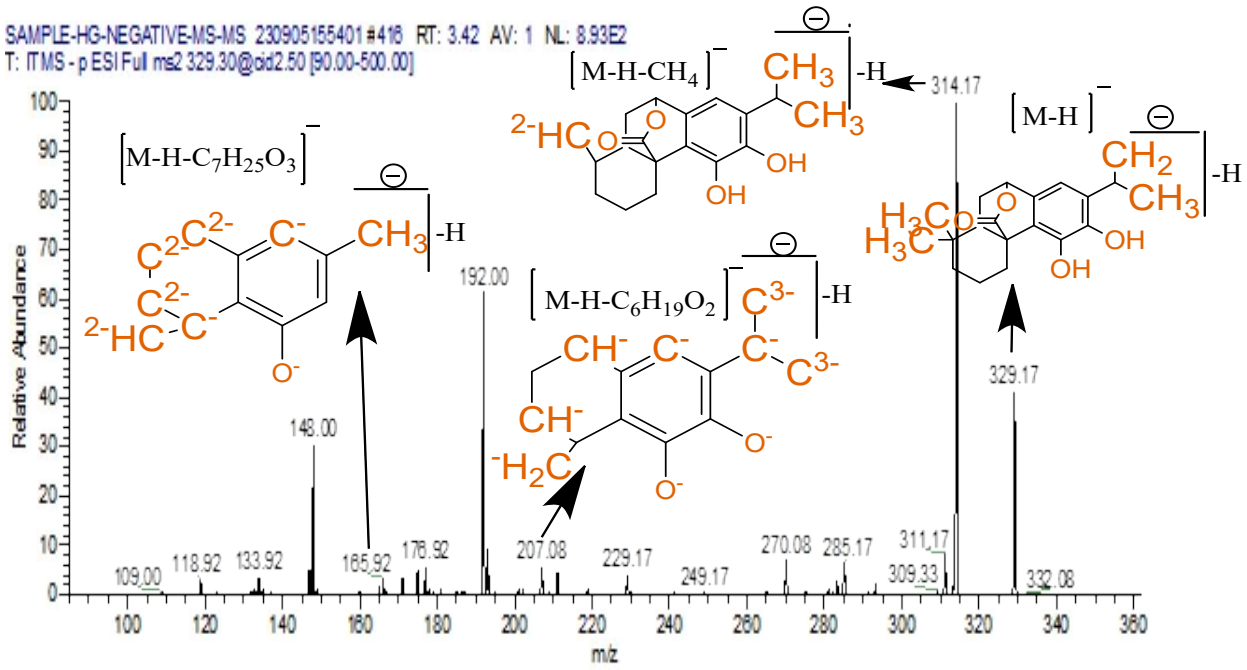

Figure S11 Comprehensive MS-MS scale of Carnosol determined applying $[M-H]^-$ ions

The product-ion peak at m/z 359.33 $[M-H]^-$ $C_{18}H_{16}O_8$ was determined as Rosmarinic acid in the mass scale of the -ve ionization approach. The MS/MS scale exhibited the fragmentation of Rosmarinic acid peak at m/z 344.17 leads to removal of $[M-H-OH]^-$, at m/z 181.00 with loss of $[M-H-C_8H_3O_5]^-$, at m/z 179.00 with extermination of $[M-H-C_9H_9O_4]^-$ and at m/z 109.08 with removal of $[M-H-C_{12}H_{11}O_6]^-$ (Figure S12).

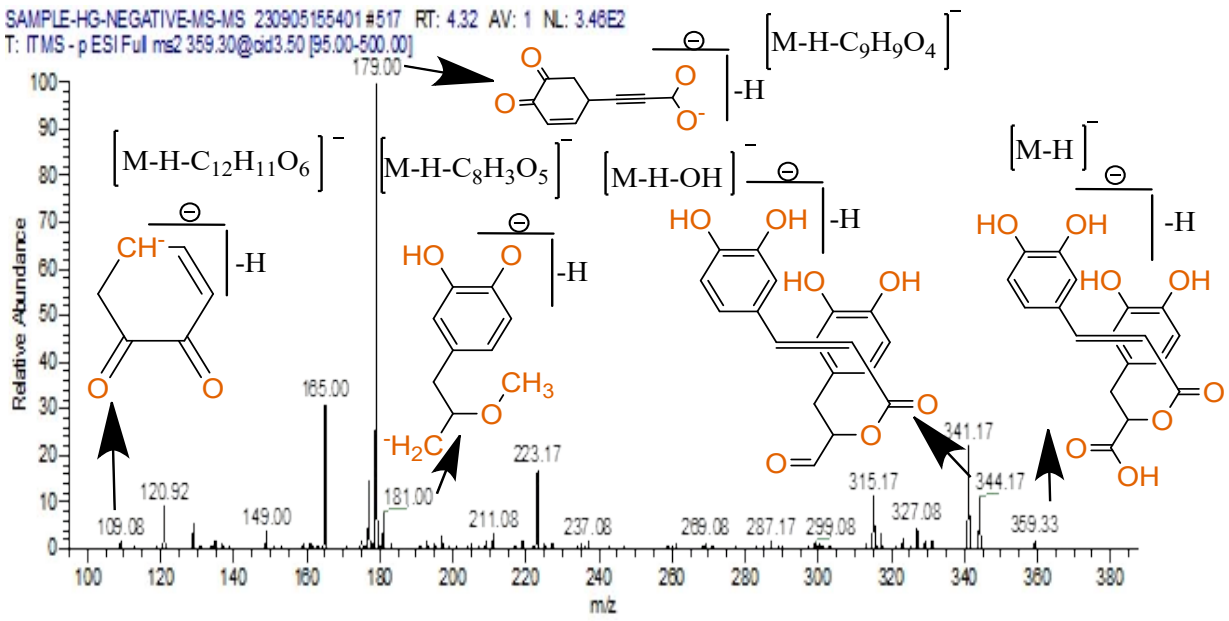

Figure S12 Comprehensive MS-MS scale of Rosmarinic acid provoked utilizing $[M-H]^-$ ions

The ion peak of molecules at m/z 435.33 $[M-H]^-$ $C_{27}H_{30}O_5$ was pointed out as Nesodine in the mass range of the -ve ionization approach. The MS/MS scale exhibited the fragmentation of the Nesodine peak at m/z 373.25, corresponding to the removal of $[M-H-C_3H_9O]^-$, at m/z 152.92 with loss of $[M-H-C_{17}H_{14}O_4]^-$ and at m/z 150.83 with extermination of $[M-H-C_{17}H_{16}O_4]^-$ (Figure S13).

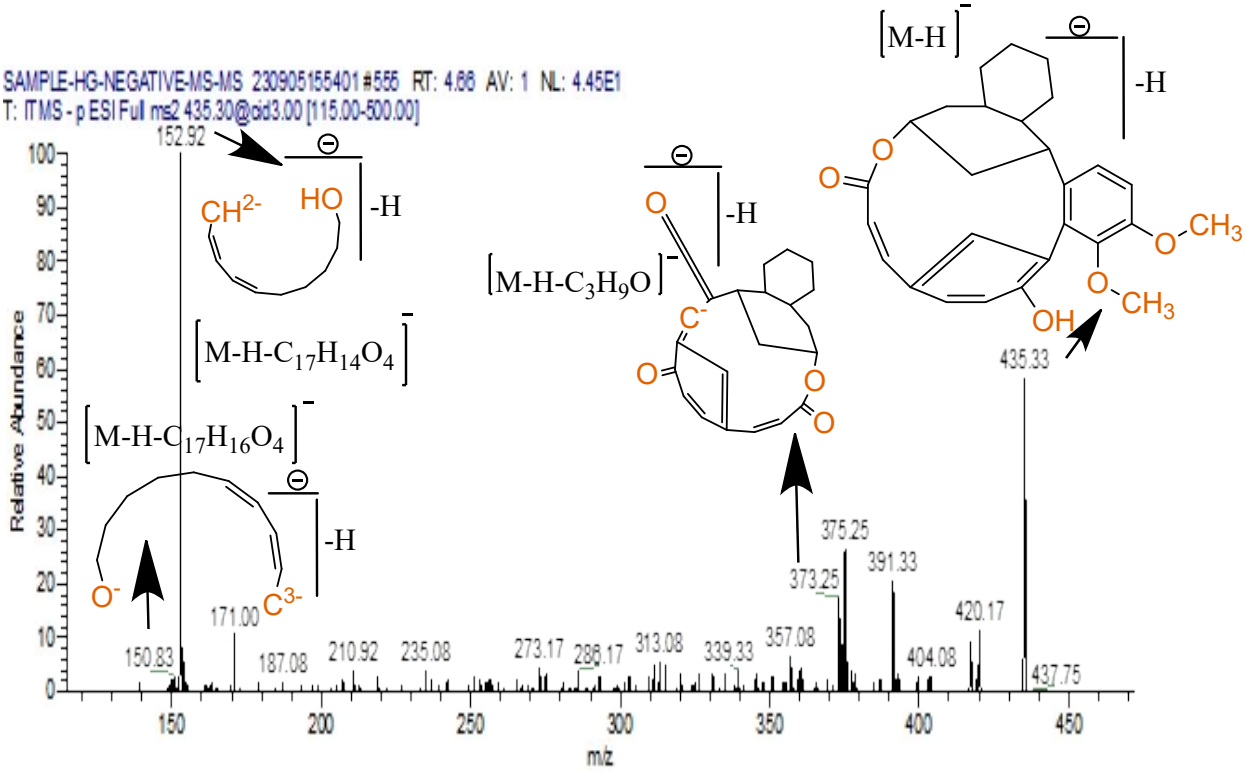

Figure S13 Comprehensive MS/MS scale of Nesodine determined using $[M-H]^-$ ions

The ion peak of precursors at m/z 505.25 $[M-H]^-$ $C_{24}H_{25}O_{12}$ was revealed as 6-O-Malonyl-rhaponticin in the mass scale of the -ve ionization approach. The MS/MS scale exhibited the fragmentation of 6-O-Malonyl-rhaponticin peak at m/z 445.25 correspond to the removal of $[M-H-CO_3]^-$, at m/z 359.25 with loss of $[M-H-C_3O_5]^-$, at m/z 325.25 with the extermination of $[M-H-C_5H_8O_7]^-$ and m/z 249.08 with the removal of $[M-H-C_{11}H_{12}O_7]^-$ (Figure S14). also described by Jiang et al and Jahan et al. [4,5].

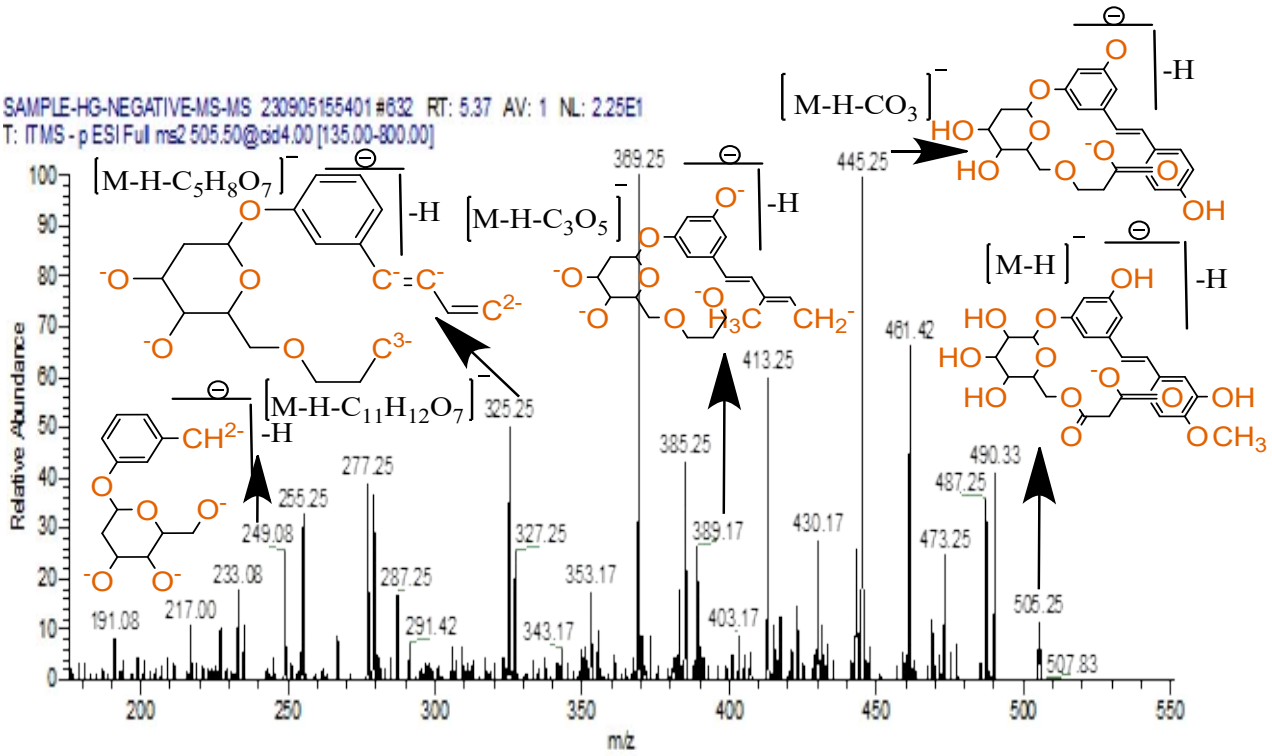

Figure S14 Comprehensive MS/MS scale of 6-O-Malonyl-rhaponticin determined utilizing [M-H]$^-$ ions

LC-ESI/MS-MS method of Total extract of Flavonoid of PP in +ve Ionization approach

The flavonoids extracted from PP in the +ve ionization approach are shown in Table 8. These flavonoids include 10-Gingerol, 6-Gingerol, Cyanidin-3-O-xyloside, 3,5-diacetoxy-7-(3,4-dihydroxy-5-methoxyphenyl)-1-(4-hydroxy-3, 5-dimethoxyphenyl) heptane, Delphinidin-3,5-O-diglucoside, 1,7-bis(3,4-dihydroxyphenyl) heptane-3,5-diyldiacetate, Diacetoxy-[4]-gingerdiol, p-cumárico acid, Diacetoxy-[6]-gingerdiol and Malvidin-3,5-O-diglucoside.

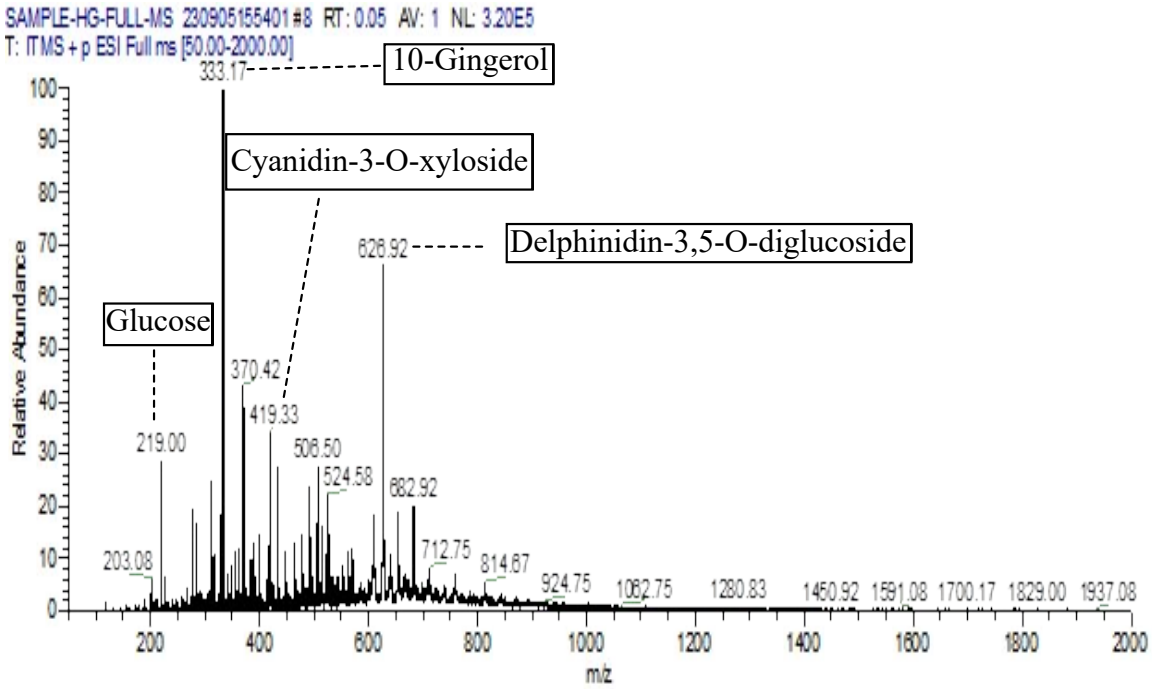

Figure S15 Comprehensive MS scale of total extract of flavonoid from PP determined utilizing $[M+H]^+$ ions

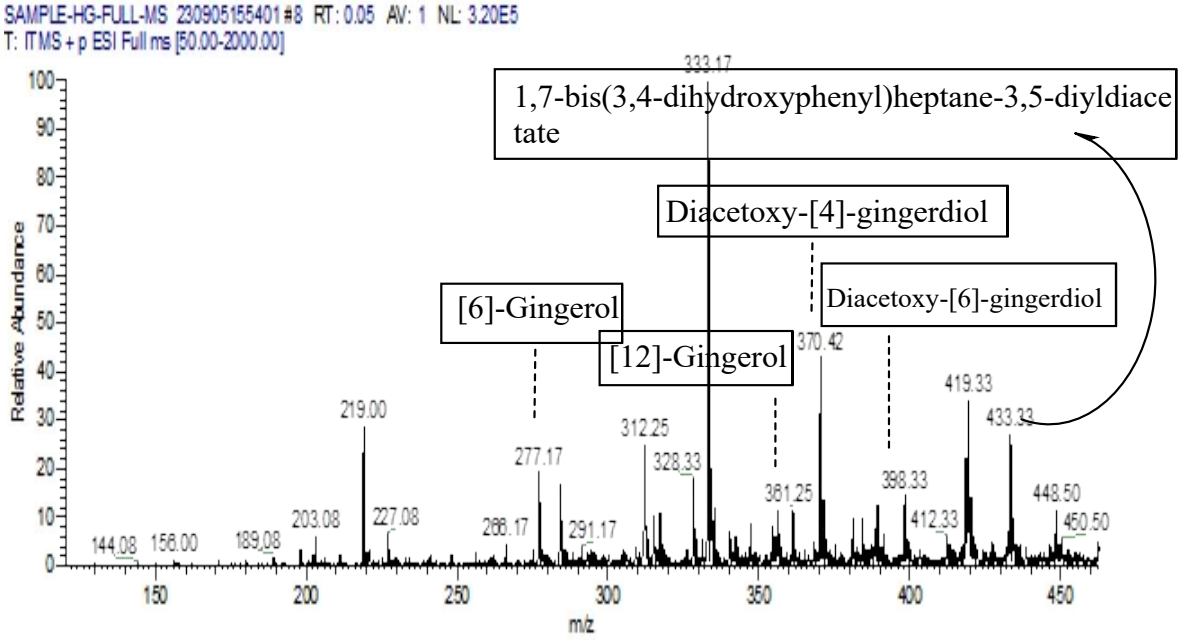

Figure S16 Comprehensive MS scale of total extract of flavonoid from PP determined utilizing $[M+H]^+$ ions

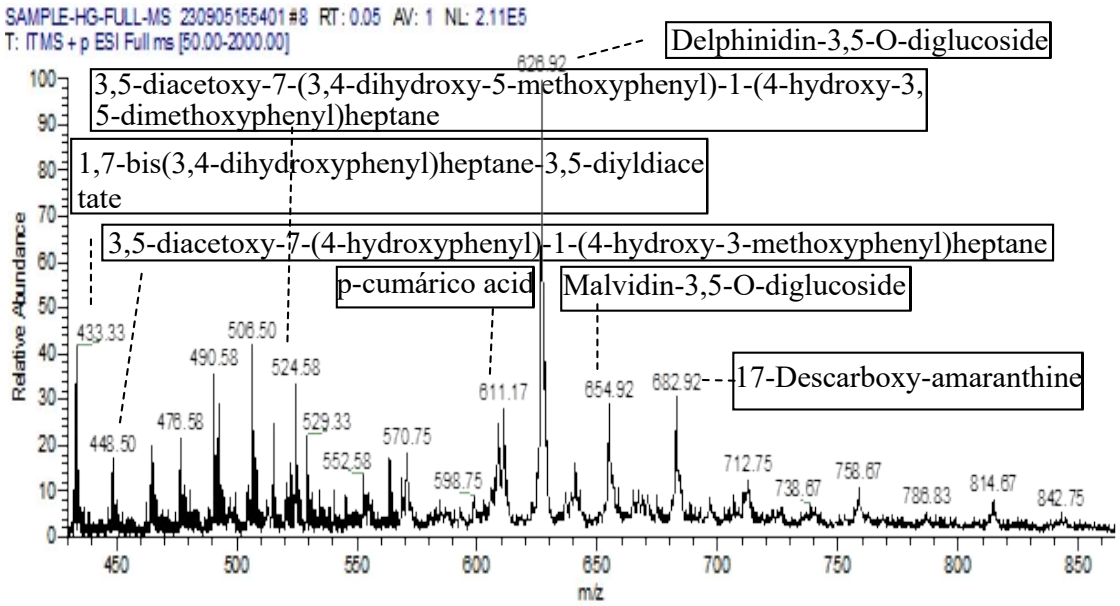

Figure S17 Comprehensive MS scale of total extract of flavonoid from PP determined utilizing $[M+H]^+$ ions

The LC/ESI/MS/MS scale in the +ve ionization approach showed a peak at m/z 118.00 $[M+H]^+$ C_9H_{10} was pointed out as Allylbenzene. It showed a precursor ion peak at m/z 103.00 corresponding to the removal of $[M+H-CH_5]^+$ and at mass/charge 58.00 by the removal of $[M+H-C_5H_2]^+$ (Figure S8).

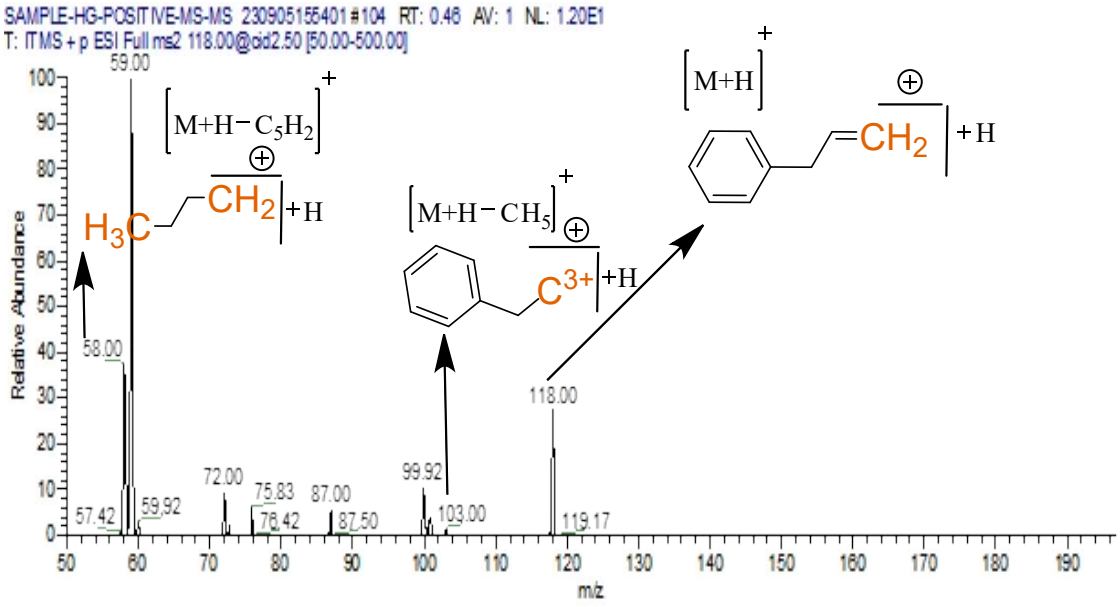

Figure S18 Comprehensive MS/MS scale of Allylbenzene determined using $[M+H]^+$ ions

The ion peak of the precursor at m/z 189.17 $[M+H]^+$ $C_{10}H_{20}O_3$ was identified as 5-Hydroxydecanoic acid in the mass scale of the +ve ionization approach. The MS/MS range exhibited the fragmentation of 5-Hydroxydecanoic acid peak at m/z 174.00 due to removal of $[M+H-CH_4]^+$ and at m/z 145.00 with loss of $[M+H-C_3H_7O_3]^+$ (Figure S19).

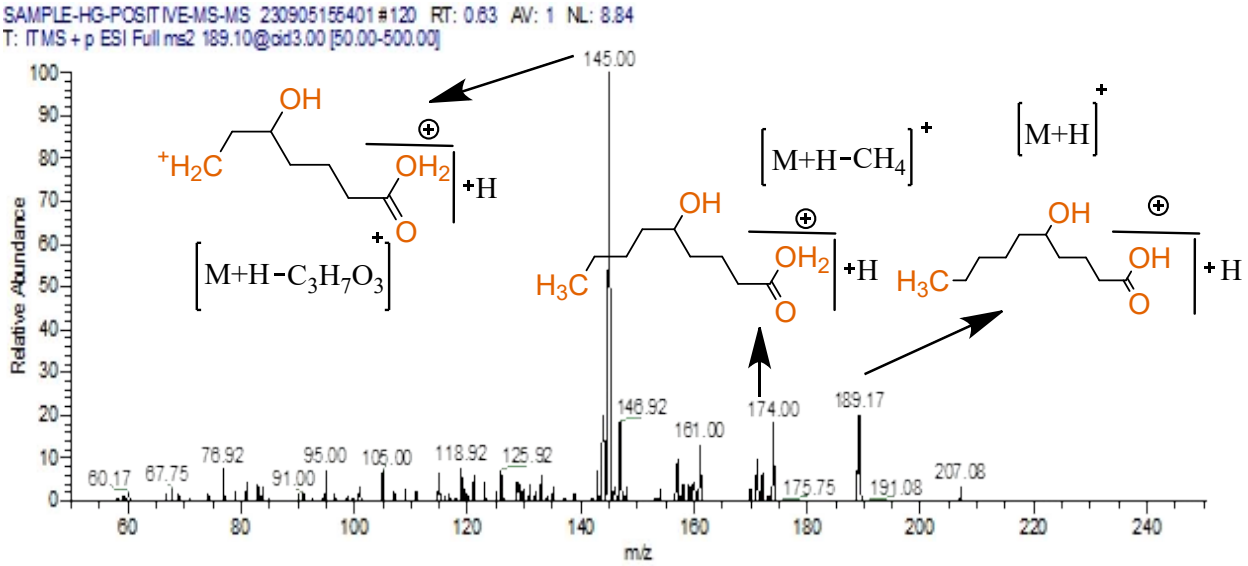

Figure S19 Comprehensive MS/MS range of 5-Hydroxydecanoic acid determined using $[M+H]^+$ ions

The ion peak of the product at m/z 203.08 $[M+H]^+$ $C_{15}H_{22}$ was pointed out as Cuparene in the mass spectrum of the +ve ionization approach. The MS/MS scale exhibited the fragmentation of the Cuparene peak at m/z 171.00, corresponding to the extermination of $[M+H-C_2H_7]^+$ and at m/z 147.00 by the extermination of $[M+H-C_4H_7]^+$ (Figure S20).

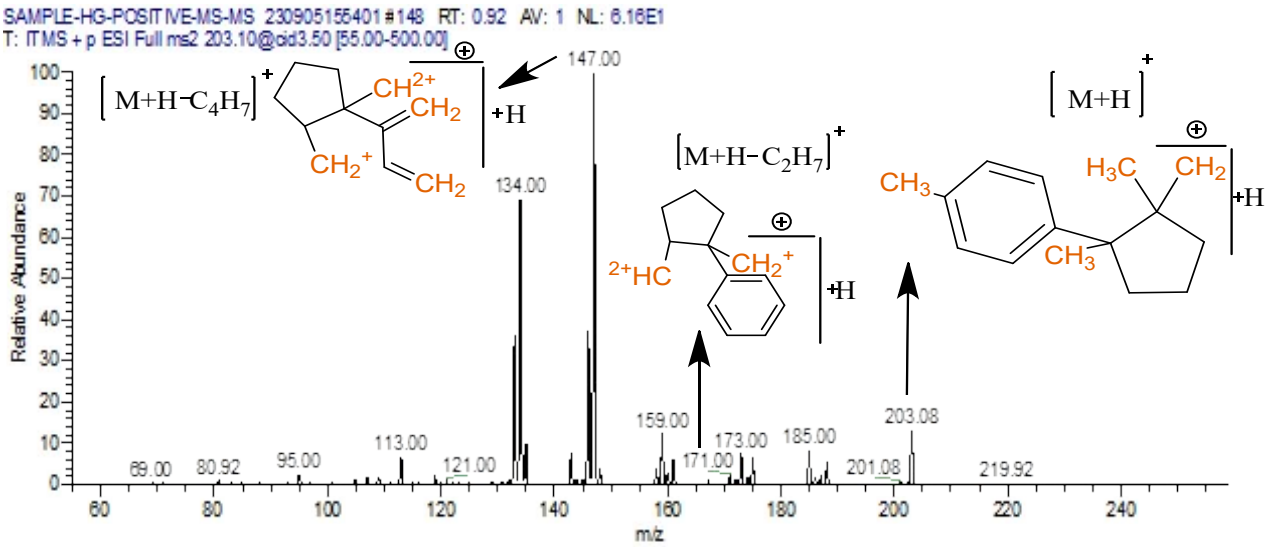

Figure S20 Comprehensive MS/MS spectra of Cuparene provoked using $[M+H]^+$ ions

The LC/ESI/MS/MS spectrum in the +ve ionization approach showed a peak at m/z 219.08 $[M+H]^+$ $C_6H_{12}O_6$ was determined as Glucose and showed precursor ion peak at m/z 163.00 correspond to removal of $[M+H\text{-}OH]^+$ and at m/z 148.00 by the extermination of $[M+H\text{-}CH_3]^+$ (Figure S21).

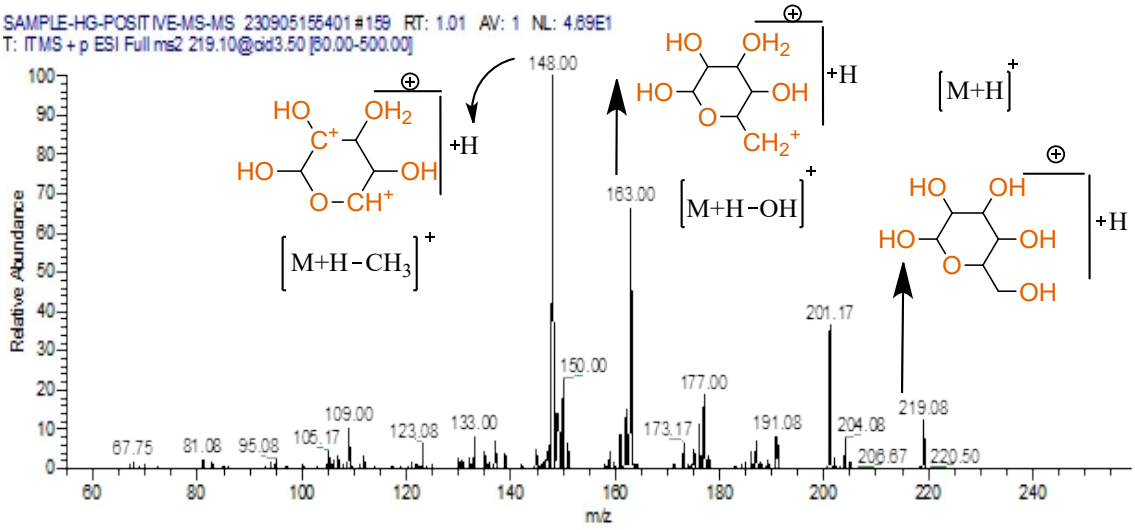

Figure S21 Comprehensive MS/MS scale of Glucose produced using $[M+H]^+$ ions

The peak appearance at m/z 312.25 $[M+H]^+$ $C_{19}H_{21}NO_5$ was assigned as Trimethylcolchicinic acid in the mass scale of the +ve ionization approach. The MS/MS scale exhibited the fragmentation of the Trimethylcolchicinic acid peak at m/z 284.17, corresponding to the extermination of $[M+H\text{-}C_2H_3NO_2]^+$ and at m/z 228.17 by the removal of $[M+H\text{-}C_5H_6NO_2]^+$ (Figure S22).

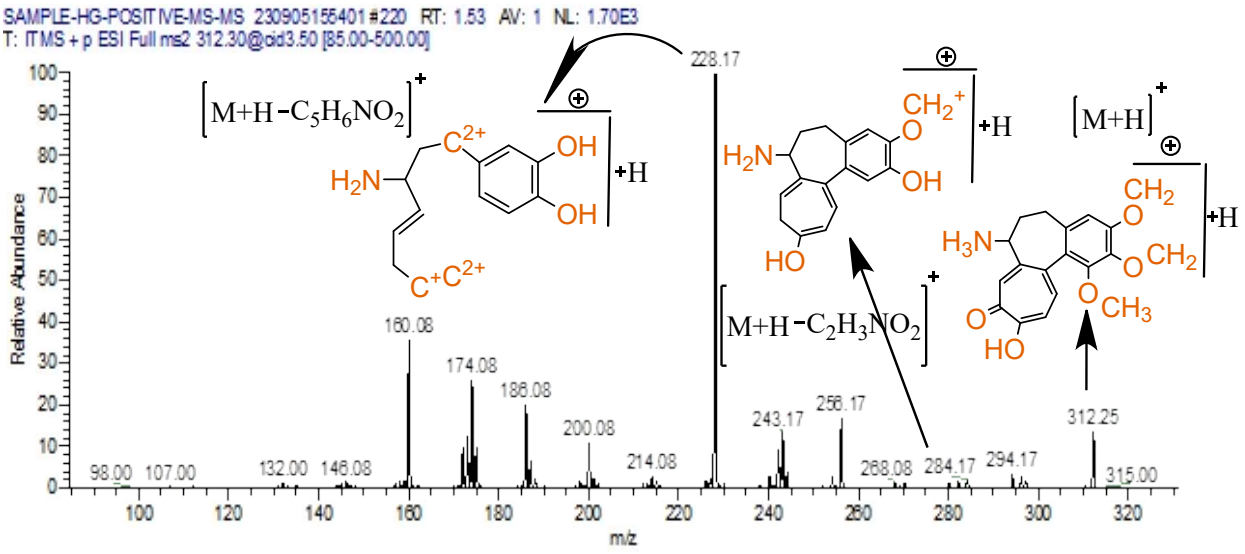

Figure S22 Comprehensive MS-MS spectra of Trimethylcolchicinic acid provoked utilizing $[M+H]^+$ ions

The ion peak of the product at m/z 333.17 $[M+H]^+$ $C_{21}H_{34}O_4$ was determined as 10-Gingerol in the mass scale of the +ve ionization approach. The MS/MS scale revealed the fragmentation of the 10-Gingerol peak at m/z 315.08 corresponds to the extermination of $[M+H-CH_7O]^+$ and at m/z 235.00 by the removal of $[M+H-C_5H_7O_3]^+$ from parent ion (Figure S23).

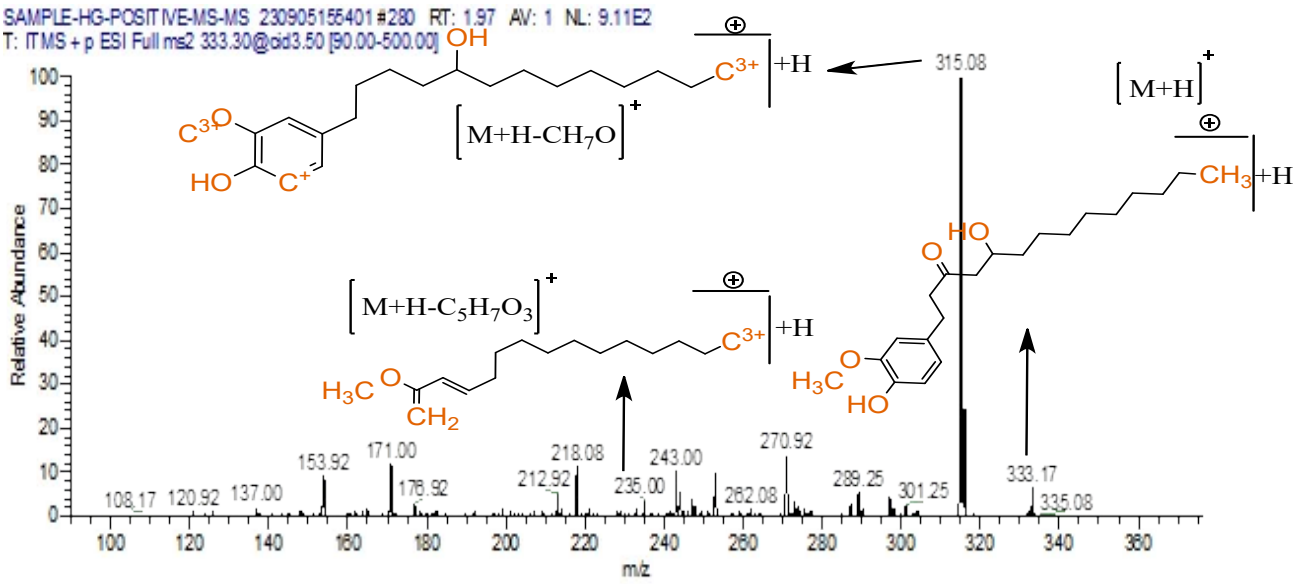

Figure S23 Comprehensive MS/MS scale of 10-Gingerol provoked using $[M+H]^+$ ions

The fragment peak of the ion at m/z 347.25 $[M+H]^+$ $C_{20}H_{26}O_5$ was pointed out as Rosmanol in mass spectra of the +ve ionization approach. The MS/MS scale showed the fragmentation of the Rosmanol peak at m/z 291.08, corresponding to the removal of $[M+H-C_3H_3O]^+$ at m/z 257.08 by the loss of $[M+H-C_3H_5O_3]^+$ and at m/z 140.92 by the removal of $[M+H-C_9H_{18}O_5]^+$ (Figure S24).

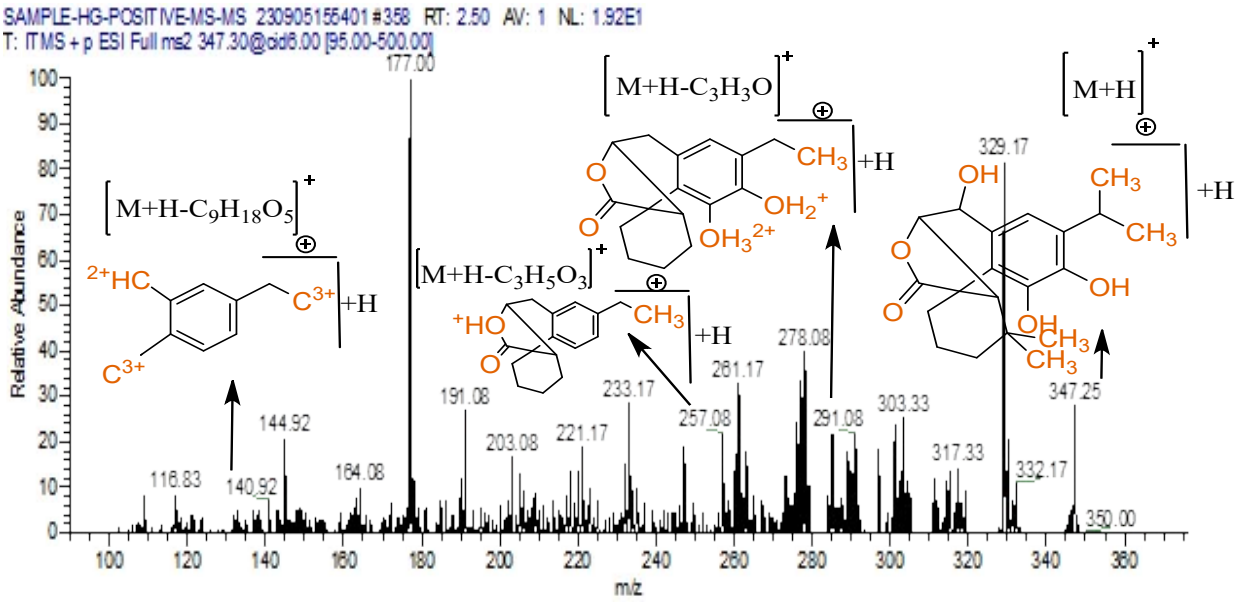

Figure S24 Comprehensive MS-MS spectra of Rosmanol produced utilizing $[M+H]^+$ ions

The mass scale with the precursor ion peak at m/z 317.25 [M+H]+ C16H12O7 was assigned as Rhamnetin, which exhibited an MS/MS scale with a peak of the daughter ion at m/z 299.17 corresponding to the removal of $[M+H-OH]^+$ and at m/z 237.08 by the extermination of $[M+H-CH_3O_4]^+$ (Figure S25).

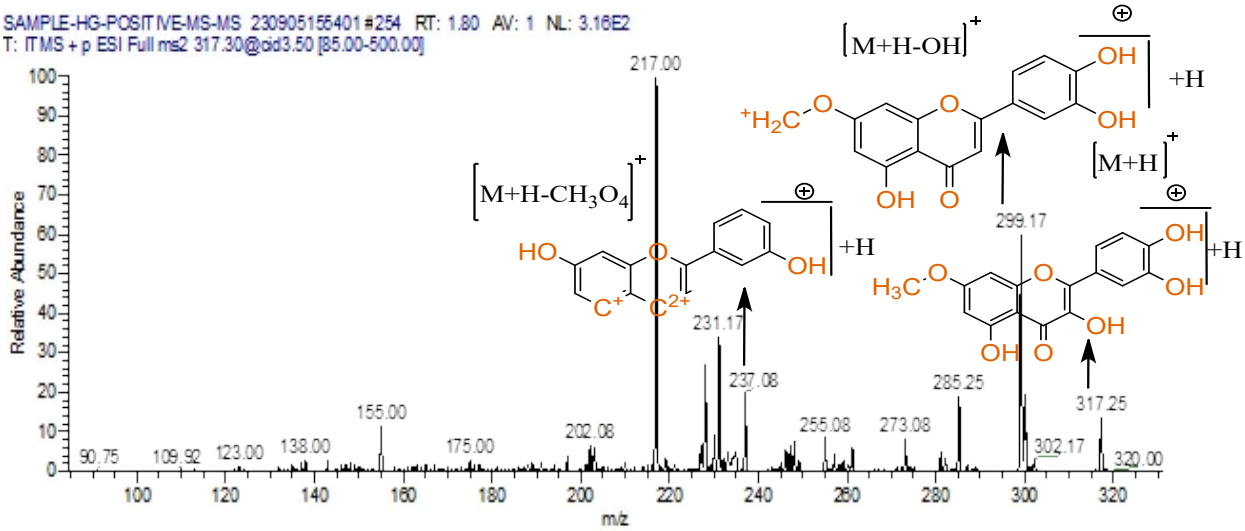

Figure S25 Comprehensive MS/MS range of Rhamnetin determined utilizing $[M+H]^+$ ions

The mass scale with fragment ion peak at m/z 419.25 $[M+H]^+$ $C_{20}H_{19}ClO_{10}$ was termed as cyanidin 3-arabinoside, which exhibited MS/MS range with daughter ion peak at m/z 351.33 corresponding

to loss of $[M+H-O_4H_4]^+$ and at m/z 210.08 by the extermination of $[M+H-C_9H_5O_6]^+$ from parent ion (Figure S26).also previously described. [7].

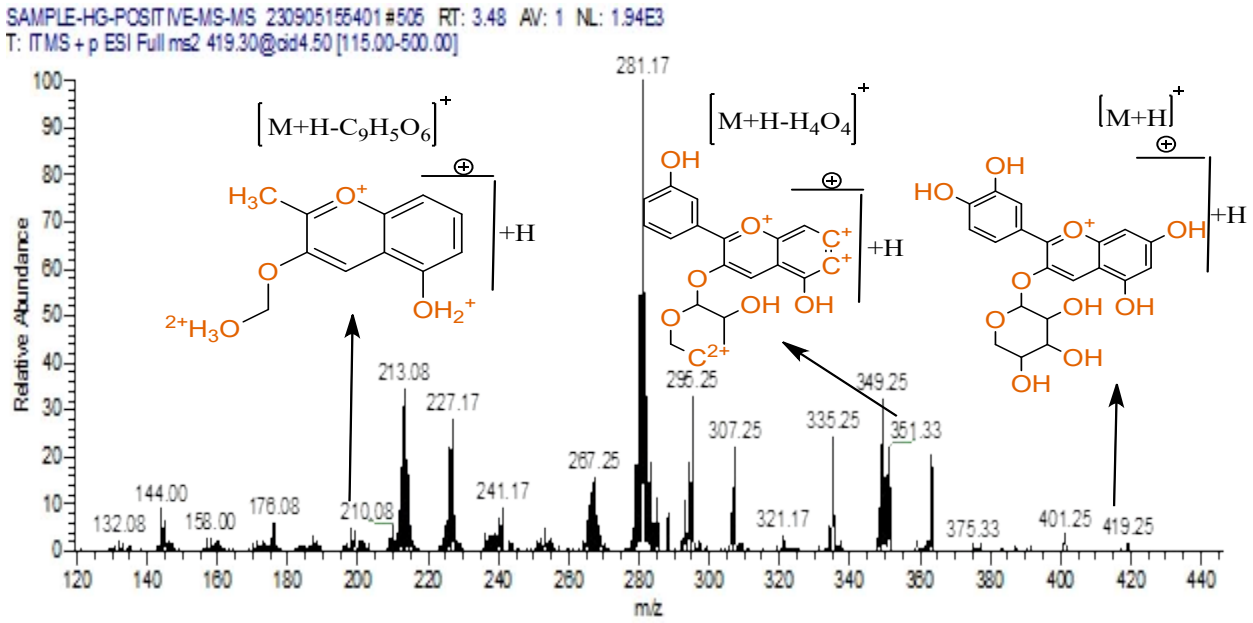

Figure S26 Comprehensive MS/MS scale of Cyanidin 3-arabinoside provoked utilizing $[M+H]^+$ ions

The peak of the daughter ion at m/z 640.42 $[M+H]^+$ $C_{29}H_{36}O_{16}$ was determined as Plantamajoside in the mass scale of the +ve ionization approach. The MS/MS scale revealed the fragmentation of the Plantamajoside peak at m/z 554.50 correspond to removal of $[M+H-C_3H_2O_3]^+$, at m/z 462.33 by the removal of $[M+H-C_5H_6O_7]^+$ and at m/z 354.25 by the extermination of $[M+H-C_9H_{18}O_{10}]^+$ from parent ion (Figure S27).

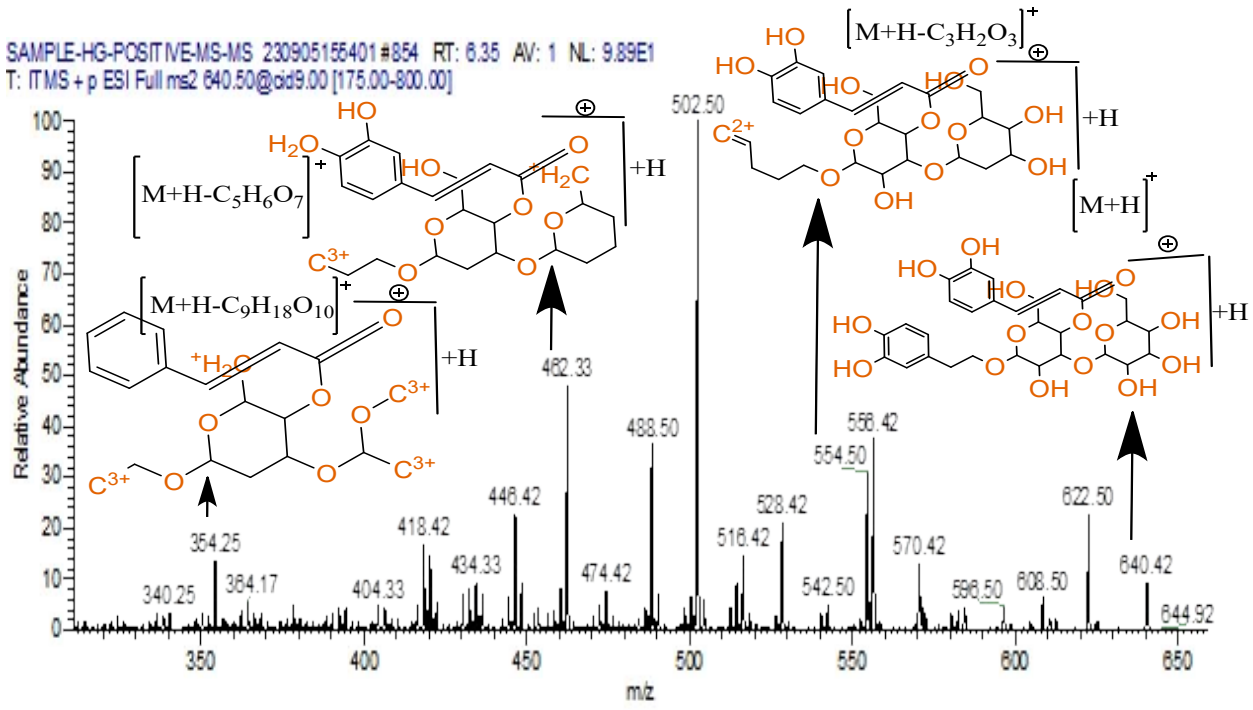

Figure S27 Comprehensive MS/MS scale of Plantamajoside determined utilizing $[M+H]^+$ ions

A peak at 712.58 was pointed out as $[M+H]^+$ $C_{39}H_{52}O_{12}$ Stelleralide A in the MS/MS mass scale with daughter ion peak at m/z 694.58 corresponding to loss of $[M+H-H_2O]^+$, at m/z 569.50 by the removal of $[M+H-C_6H_7O_4]^+$ and at m/z 408.33 by the removal of $[M+H-C_{14}H_8O_8]^+$ from parent ion (Figure S28).

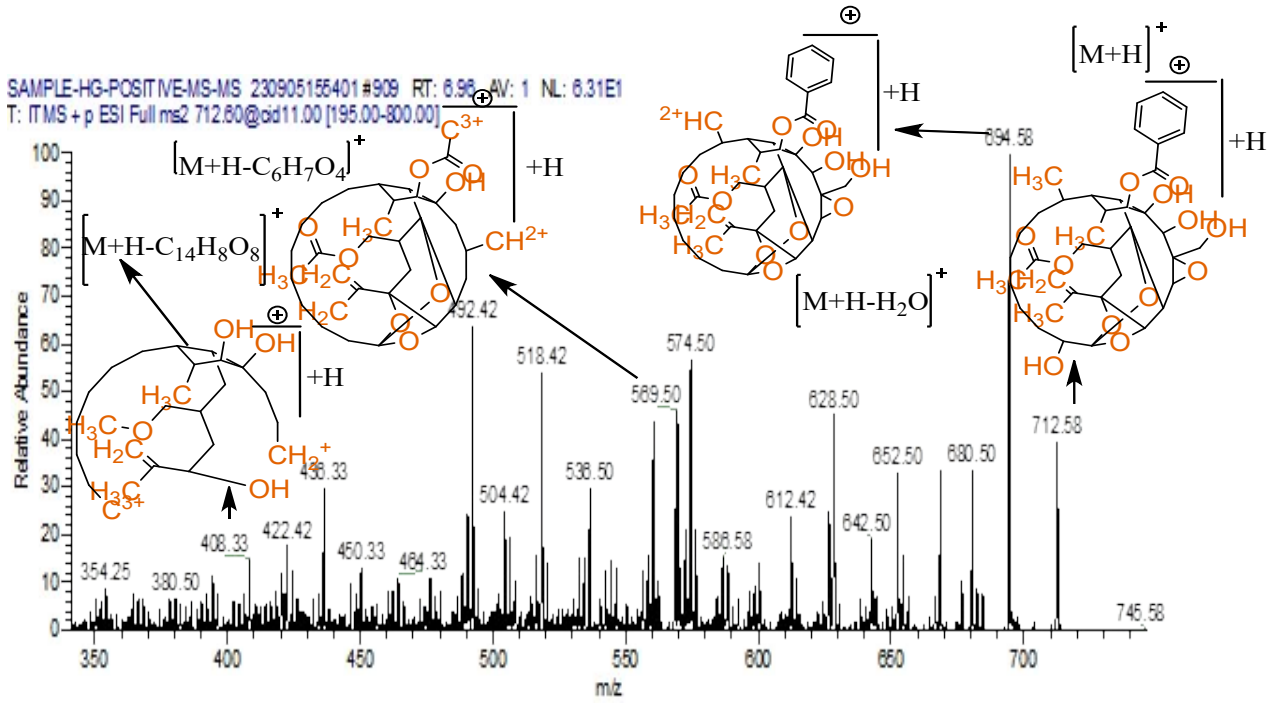

Figure S28 Comprehensive MS/MS scale of Stelleralide A produced operating $[M+H]^+$ ions

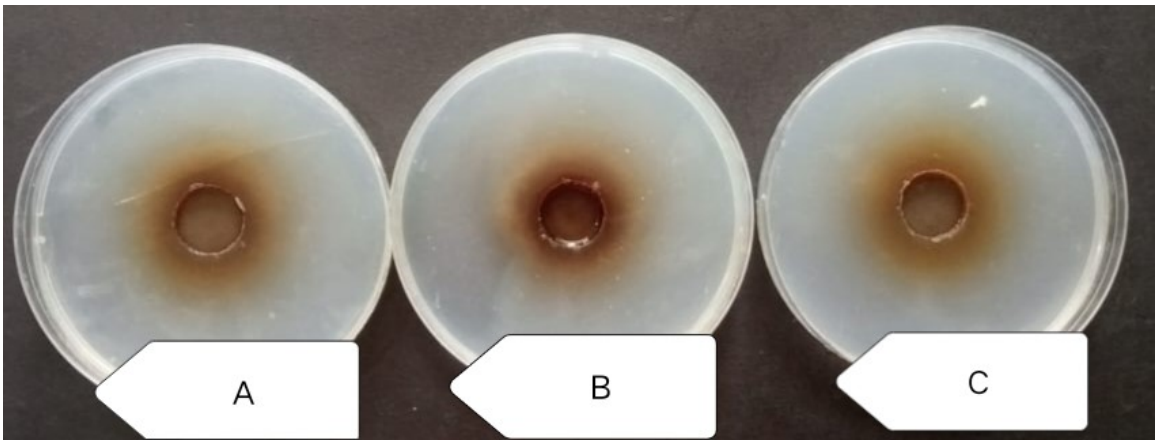

Figure S29. Zone of inhibition of PP extract against *Pseudomonas syringae* at a concentration (A) 50mg/mL, (B) 100mg/mL, (C) 150mg/mL

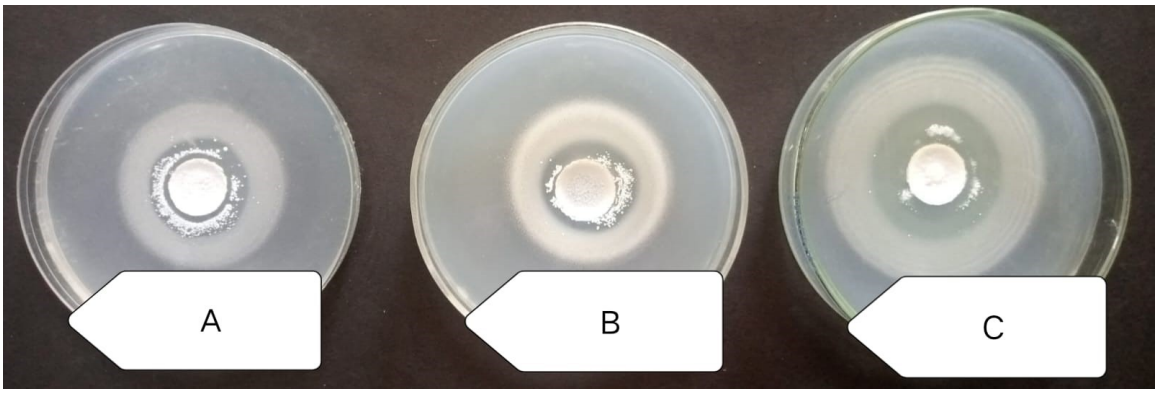

Figure S30. Zone of inhibition of Ciprofloxacin against *Pseudomonas syringae* at different concentrations (A) 50mg/mL, (B) 100mg/mL, (C) 150mg/mL

Figure S31 Inhibition zone of PP extract against *Clavibacter michiganensis* at different concentrations of extract (A) 50mg/mL, (B) 100mg/mL, (C) 150mg/mL

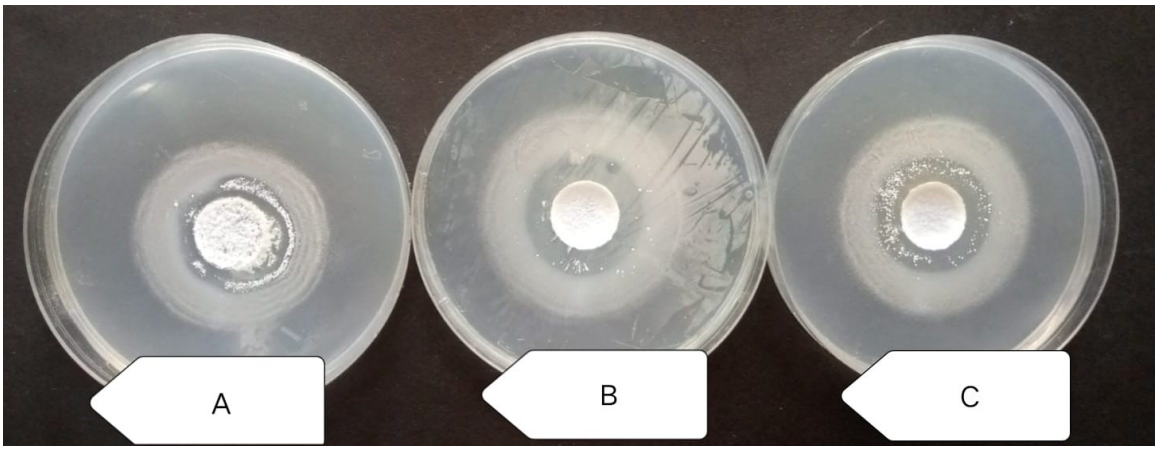

Figure S32 Inhibition zone of Ciprofloxacin against *Clavibacter michiganensis* at different concentrations of extract (A) 50mg/mL, (B) 100mg/mL, (C) 150mg/mL.

Figure S33 Zone of inhibition of PP extract against *Aspergillus niger* at varying concentrations of extract (A)150mg/mL, (B) 100mg/mL, (C) 50mg/mL

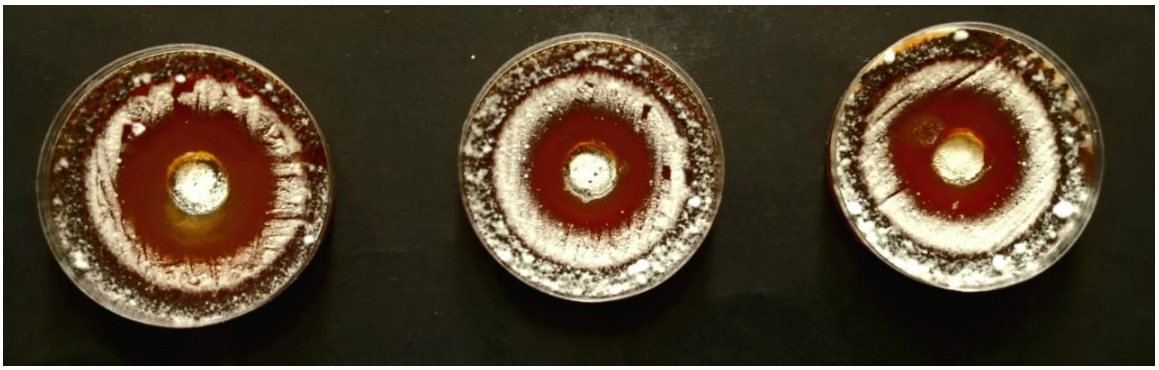

Figure S34 Zone of inhibition of Fluconazole against *Aspergillus niger* at different ranges of dosage of extract (A) 50mg/mL, (B) 100mg/mL, (C) 150mg/mL.

Figure 35 Inhibition zone of *Zingiber officinale* mediated extract against *Alterneria alternata* at different concentrations of extract (A) 50mg/mL, (B) 100mg/mL, (C) 150mg/mL

Figure S36 Zone of inhibition of Fluconazole against *Alterneria alternata* at different dosages of extract (A) 50mg/mL, (B) 100mg/mL, (C) 150mg/mL

Tables

Table S1 Compound name and compounds' anatomy determined from the PP extract in -ve ionization approach.

Sr No	**Compound**	**Compound's structure**	**Sr No**	**Compound**	**Compound's structure**
1	3,7-Dimethylquercetin	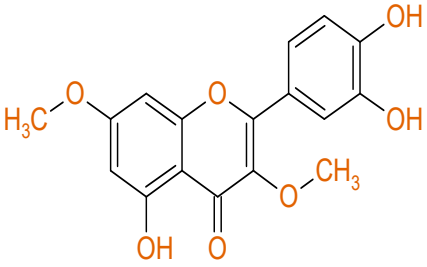	7	Malic acid	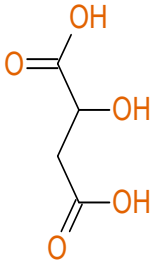

2	Kaempferol-3-O-desoxyhexoside	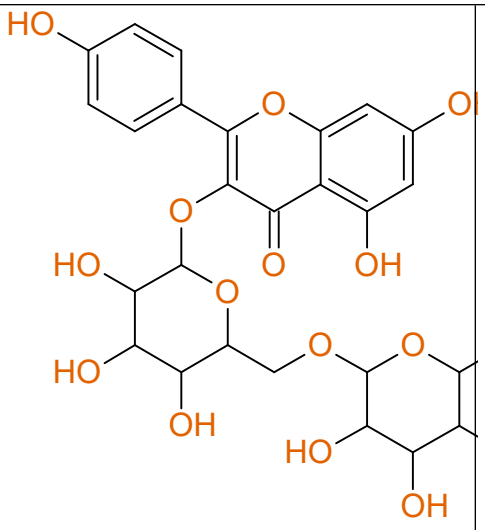	8	3'-Hydroxydaidzein	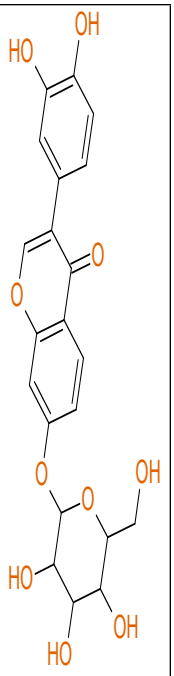
3	Chrysoeriol-7-O-glycuronyl	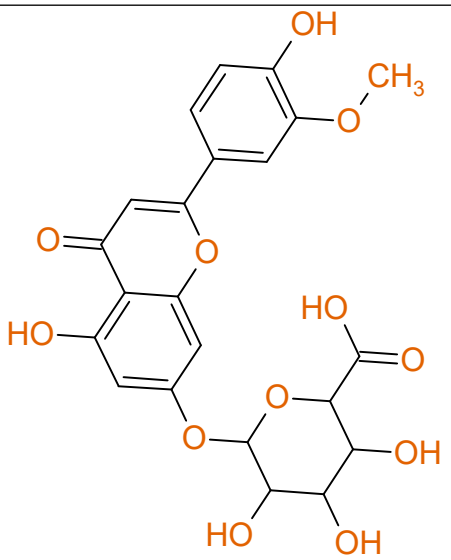	9	3,7-Dimethylquercetin	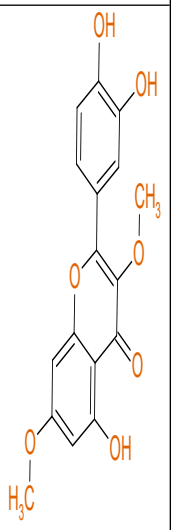

4	Quercetin-3-malonylglucoside	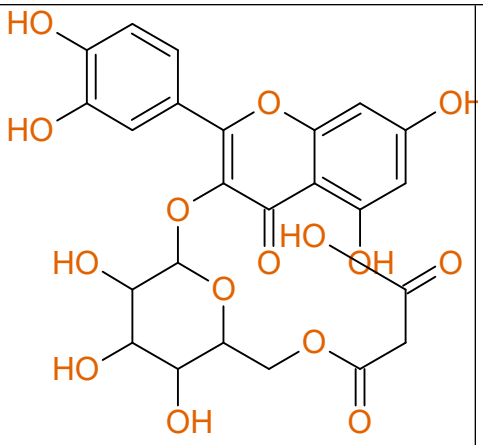	10	Ferulic acid	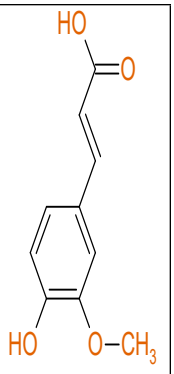
5	Cafeic acid	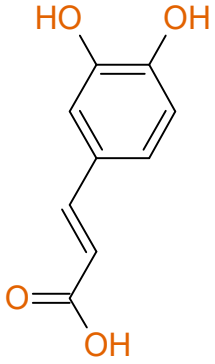	11	Umbelliferone	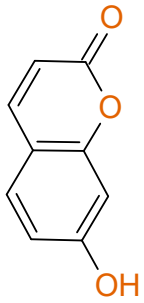
6	[6]-gingerol	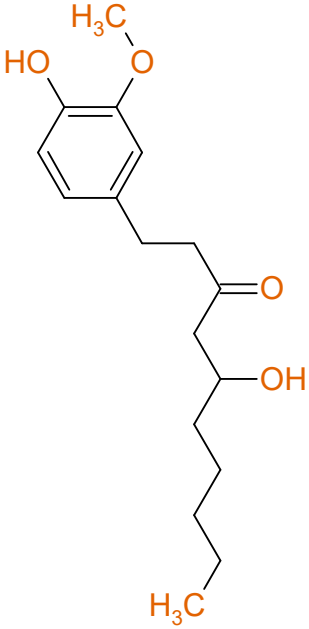	12	Glucose	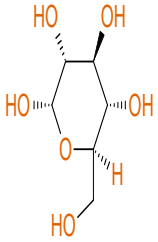

Table S2 Compound name and structure of compounds determined from the emulsion of PP in +ve ionization approach.

Sr No	Compound	Compound structure	Sr No	Compound	Compound structure
1	10-Gingerol	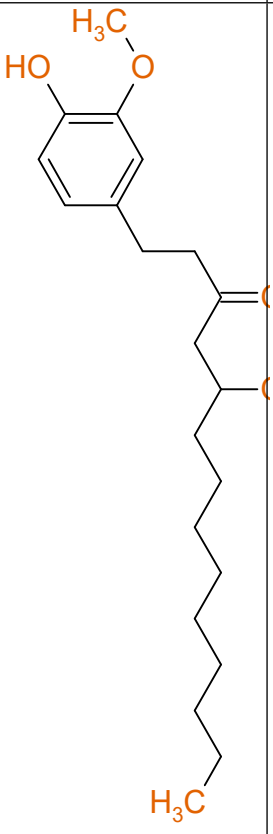	6	[6]-Gingerol	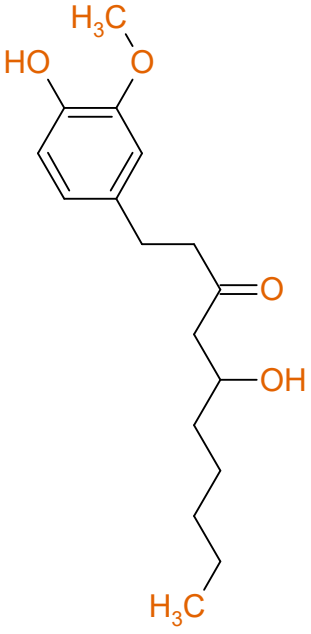
2	Cyanidin-3-O-xyloside	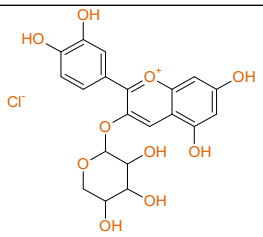	7	3,5-diacetoxy-7-(3,4-dihydroxy-5-methoxyphenyl)-1-(4-hydroxy-3, 5-dimethoxyphenyl)heptane	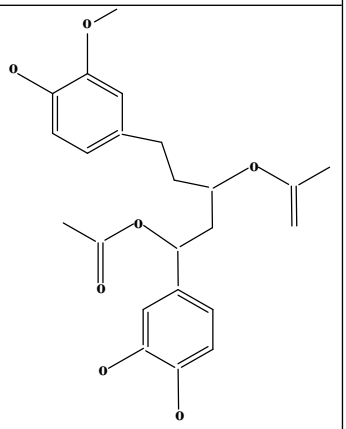

3	Delphinidin-3,5-O-diglucoside	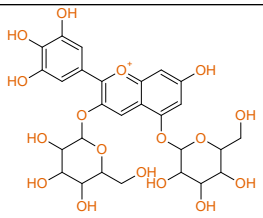	8	1,7-bis(3,4-dihydroxyphenyl)heptane-3,5-diyldiacetate	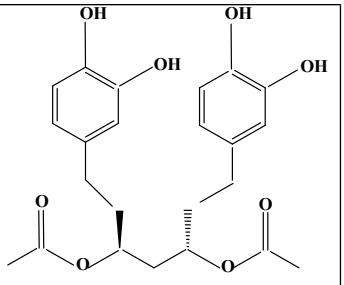
4	Diacetoxy-[4]-gingerdiol	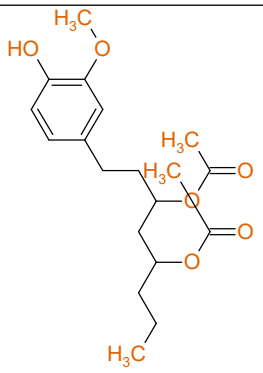	9	p-cumárico acid	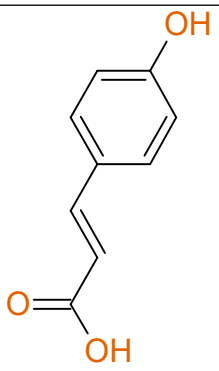
5	Diacetoxy-[6]-gingerdiol	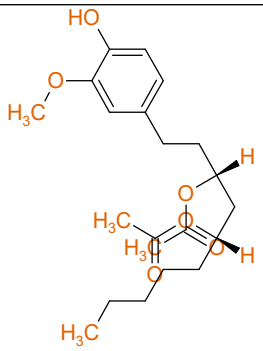	10	Malvidin-3,5-O-diglucoside	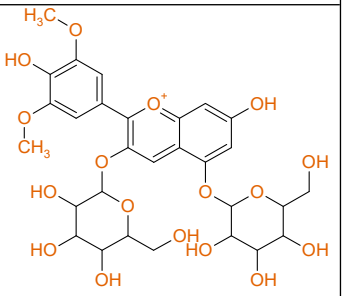

1. **!!! INVALID CITATION !!! [100-103]**.
2. Jiang, H.; Sólyom, A.M.; Timmermann, B.N.; Gang, D.R.J.R.C.i.M.S.A.I.J.D.t.t.R.D.o.U.t.t.M.R.i.M.S. Characterization of gingerol-related compounds in ginger rhizome (Zingiber officinale Rosc.) by high-performance liquid chromatography/electrospray ionization mass spectrometry. **2005**, *19*, 2957-2964.

3. Tao, Y.; Li, W.; Liang, W.; Van Breemen, R.B.J.J.o.a.; chemistry, f. Identification and quantification of gingerols and related compounds in ginger dietary supplements using high-performance liquid chromatography− tandem mass spectrometry. **2009**, *57*, 10014-10021.
4. Jahan, N.; Hussian, F.; Ayub, A.R.; Ilyas, M.; Khan, M.A.; Manzoor, R.; Khan, W.A.J.C.P. Isolation and characterization of flavonoids from roots of Rauvolfia serpentina and evaluation of their hypotensive potential through angiotensin-converting enzyme (ACE) inhibition mode of action. **2022**, *76*, 5133-5143.
5. Jiang, H.; Timmermann, B.N.; Gang, D.R.J.R.C.i.M.S.A.I.J.D.t.t.R.D.o.U.t.t.M.R.i.M.S. Characterization and identification of diarylheptanoids in ginger (Zingiber officinale Rosc.) using high-performance liquid chromatography/electrospray ionization mass spectrometry. **2007**, *21*, 509-518.
6. **!!! INVALID CITATION !!! [100, 101, 107, 108]**.
7. Zubair, M.S.; Maulana, S.; Widodo, A.; Pitopang, R.; Arba, M.; Hariono, M.J.M. GC-MS, LC-MS/MS, docking and molecular dynamics approaches to identify potential SARS-CoV-2 3-chymotrypsin-like protease inhibitors from Zingiber officinale Roscoe. **2021**, *26*, 5230.